IEEE Access
Multidisciplinary | Rapid Review | Open Access Journal

SPECIAL SECTION ON URBAN COMPUTING AND INTELLIGENCE

Received August 10, 2019, accepted August 26, 2019, date of publication September 17, 2019,
date of current version September 25, 2019.

Digital Object Identifier 10.1109/ACCESS.2019.2939718

Photovoltaic Modules Monitoring Based on WSN With Improved Time Synchronization

XIANBO SUN[1,2], YIXIN SU[1], YONG HUANG[2], JIANJUN TAN[2], JINQIAO YI[2], TAO HU[2], AND LI ZHU[2]

[1]School of Automation, Wuhan University of Technology, Wuhan 430070, China
[2]School of Information Engineering, Hubei Minzu University, Enshi 445000, China

Corresponding author: Yixin Su (suyixin@whut.edu.cn)

This work was supported in part by the National Natural Science Foundation of China under Grant 61561020 and Grant 61661020.

ABSTRACT In order to avoid clock skew in WSN (Wireless Sensor Networks) for large-scale photovoltaic modules monitoring, an improved time synchronization algorithm, TSP-GDM (Time Synchronization Protocol with Gaussian Delay Model) is proposed in this paper. Interdependence of local time stamps is established between network nodes according to a linear clock model. Local exchange and share of local time stamps in nodes are achieved by means of wireless transmission. An estimation method with the Gaussian Delay Model is designed to deal with the estimation problems of the node clock offset. The synchronization accuracy of the proposed method is verified with the MATLAB simulation. It is found that TSP-GDM can be applied to synchronous topology of large-scale photovoltaic modules monitoring with a higher synchronization accuracy. Compared to RBS (Reference Broadcast Synchronization), TPSN (Timing-synchronization Protocol for Sensor Networks) and RTSP (Recursive Time-Sync Protocol for WSN), its synchronization accuracy in an inner layer has been increased by 22.57 μs, 15.7 μs and 4.26 μs respectively.

INDEX TERMS Gaussian delay model, photovoltaic modules monitoring, time synchronization, WSN.

I. INTRODUCTION

WSN (Wireless Sensor Networks) to photovoltaic modules monitoring is a hierarchical topology sensor network equipped with massive sensor nodes in the module monitoring sections through wireless communication [1]. The photovoltaic system consists of a large number of photovoltaic modules. Usually, those photovoltaic modules need to be divided into many groups, those modules in a group are arranged according to the star-shaped net structure and the related nodes constitute a micro wireless sensor local area network. Each micro local area network in the star-shaped net structure uses a single central node to communicate with background server through the data interface. Consequently, effective transmission of data and real-time monitoring of component status are enabled.

The monitoring data information is from different sensor nodes such as component temperature, output voltage, output current and has a close coupling relationship with the local clock of the node. This localized relationship will restrict the degree of time correlation between the sensor node data, which in turn brings about the time asynchronism of the node data, and seriously affects the analysis and judgment of the abnormal modules.

Time synchronization is one of the important supporting technologies in WSN. Many operations require accurate time synchronization, such as data fusion, node tracking and positioning, power management, transmission scheduling [2], [3]. Generally, the design of WSN time synchronization algorithm not only focuses on such relevant algorithm indexes as accuracy, energy consumption, but also needs to fully consider the specific scenarios including network topology, time synchronization requirements.

There are four main types of time synchronization methods for WSN:

The first type is the sender-receiver synchronization (SRS), such as DMTS (Delay Measurement Time Synchronization) [4], FTSP (Flooding Time Synchronization Protocol) [5], TPSN [6] and Mini-sync [7], which is flexible, lightweight and energy efficient, but its synchronization accuracy is not high. The DMTS algorithm [4] is influenced by clock accuracy and interrupt processing delay.

The associate editor coordinating the review of this manuscript and approving it for publication was Lu Liu.

The second type is receiver-receiver based synchronization (RBS) methods, such as RBS [8] and Adaptive RBS [9]. Adaptive RBS can achieve high synchronization accuracy, but the cost of synchronization message is higher when the number of nodes is larger.

The third type is only the receiver synchronization (ROS). It mainly realizes time synchronization by listening. This method sacrifices accuracy to a certain degree, but significantly reduces energy consumption.

The last type is the time synchronization method based on bionic structure, such as typical firefly synchronization algorithm and cooperative synchronization technology [10], [11].

In recent years, some researchers have improved the methods involved in the above synchronization mechanisms on two performance indicators: synchronization accuracy and synchronization energy consumption. For example, Low-power Clustering-based Time Synchronization (LCTS) algorithm proposed in [12], which combines unidirectional broadcast synchronization with bidirectional pairing synchronization, can effectively reduce energy consumption on the premise of ensuring accuracy. However, without consideration of the restriction of transmission distances between nodes, it's hard to use this method in the WSN for the photovoltaic modules monitoring. Djenouri [13] has proposed an improved RBS algorithm, Relative Reference Receiver/Receiver Time-Sync in WSN (R4-Syn). Two additional clock reference nodes are added to time synchronization, and then the frequency and phase compensation are estimated by the maximum likelihood estimation method. The synchronization accuracy and the stability of this method are superior to that of RBS algorithm. But this method faces the same problem as that of [12]. That is high complexity of overall synchronization topology construction and the mere application to small-scale time synchronization. Maggs *et al.* [14] have presented Consensus Clock Synchronization (CCS) algorithm. The virtual consensus clock CC is constructed by combining the node's reliability parameters and the clock phase compensation values of neighboring nodes. Frequency compensation value and phase compensation value which consensus clock synchronization needs to synchronize with the consensus clock are calculated according to local time stamp of every node. CCS algorithm can be applied to modules monitoring with good extensibility. However, its consumption of synchronization message is high. Because of the lack of full utilization broadcasting characteristics of wireless channels, every node needs to send at least one synchronization message. It results in a large energy consumption and a long synchronization period. The RTSP method proposed in [15] is an improved TPSN algorithm, which is synchronized with data nodes by multi-hop communication according to its own synchronization requirements.

Thus, it can be seen that the key to the typical time synchronization algorithms mentioned above lies in the estimation of clock offset. However, there are few research on WSN synchronization topology for the state monitoring of photovoltaic modules. WSN for photovoltaic modules monitoring is basically featured with: 1) hierarchy structure shown by network topology. 2) full use of the broadcast characteristics of wireless channel. 3) limitations in network resources, including node energy, calculation ability, communication bandwidth [16], [17], etc.

Therefore, a designed time synchronization algorithm for WSN in this case needs to take the following into consideration: 1) estimation method of clock offset between nodes in a monitoring area, 2) the accuracy of a time synchronization algorithm, 3) message consumption of time synchronization algorithm.

To solve the estimation problems of node clock offset for modules status monitoring, a time synchronization algorithm, TSP-GDM is proposed in this paper. Firstly, the algorithm makes full use of the wireless broadcast characteristics of monitoring nodes in WSN. It realizes the local sharing of local time stamps among nodes. It establishes the interdependence of local time stamps among nodes according to the linear clock model. Secondly, an estimation method with Gaussian Delay Model is designed to solve estimation problems of the node clock offset in the modules monitoring. Lastly, synchronization accuracy and synchronization energy consumption of this method is verified through MATLAB simulation.

II. TIME SYNCHRONIZATION MODEL UNDER THE CONDITIONS OF LINEAR CLOCK

Physical clock of WSN node is realized by counting interrupt of crystal oscillator assembled by itself. Moreover, the value of the interrupt count generated in each second is fixed under ideal state. Due to the different frequency errors and initial timing of crystal oscillator at each node, the physical clocks between nodes are inconsistent. If the potential link between physical clocks on different nodes is investigated, then the corresponding logical clocks can be constructed to achieve time synchronization.

T is defined as actual physical time, and $T(t)$ stands for local time of nodes. For an ideal clock, its time change rate $dT(t)/dt$ equals a constant 1. However, some certain drifts usually exist in crystal oscillator, so that definable time change rate offset is $(dT(t)/dt) - 1$. Assuming $f(t) = dT(t)/d\mathrm{t}$, the change of local time $T_i(t)$ of node i from physical time t_0 to t can be expressed by (1) [18].

$$\mathrm{T}_i(t) = \int_{t_0}^{t} f_i(\tau) d\tau + \psi_i(t_0) \tag{1}$$

where $\psi_i(t_0)$ is initial phase value of node i at physical time t_0. Equation (1) is expanded to following equation by Taylor series.

$$\mathrm{T}_i(t) = \beta_i + \alpha_i t + \gamma_i t^2 + \cdots \tag{2}$$

In (2), β_i and α_i represent phase offset and frequency offset with actual physical time t, respectively. If the coefficients above the quadratic term in (2) are all 0, then (2) can be simplified into linear clock model [19], as:

$$\mathrm{T}_i(t) = \beta_i + \alpha_i t \tag{3}$$

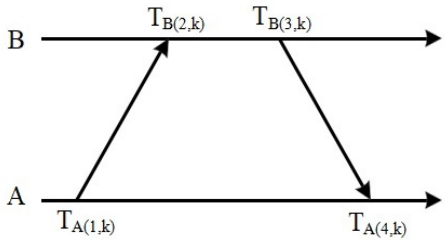

FIGURE 1. Bidirectional time stamp between the nodes exchanging information model.

Based on the linear clock model described in (3), clock relations between the nodes depend on current frequency parameter α_i and initial phase parameter β_i. When sensor nodes start up and do the regular work, parameter β_i is determined and remains unchanged while parameter α_i changes with time, which is mainly caused by the drift effect of crystal oscillator.

According to (3), the clock interdependence between two nodes A and B can be expressed as:

$$\mathrm{T}_B(t) = \beta_{AB} + \alpha_{AB} T_A(t) \tag{4}$$

In (4), β_{AB} and α_{AB} stand for phase offset and frequency offset between A and B. If and only if conditions $\beta_{AB} = 0$ and $\alpha_{AB} = 1$ hold at the same time, nodes A and B can achieve clock synchronization. Therefore, the core task of time synchronization algorithm based on linear clock model is to estimate the relative frequency offset and phase offset between the nodes.

III. ESTIMATION OF NODE CLOCK OFFSET IN MONITORING AREA

In Fig.1, the effects of clock phase offset and frequency offset on timing information interaction between nodes A and B are given. In Fig.1, after the k^{th} times information exchanges, time stamps $T_{A(1,k)}$ and $T_{A(4,k)}$ are both based on local clock of node A, while $T_{B(2,k)}$ and $T_{B(3,k)}$ are both based on the local clock of node B. Node A sends a synchronous message (including topology where node A lies in, identity number and time stamp value $T_{A(1,k)}$) to node B. After receiving the message, node B sends one confirmation message to A. Again this message includes topology of node B, the identity and time stamp values of $T_{A(1,k)}$, $T_{B(2,k)}$, $T_{B(3,k)}$. At last, node A has received this message at $T_{A(4,k)}$.

In Fig.1, $T_{A(1,1)}$ will be used as reference time ($T_{A(1,1)} = 0$), the time stamp of k^{th} uplink information about node B is $T_{B(2,k)}$, then:

$$\mathrm{T}_{B(2,k)} = (T_{A(1,k)} + d + X_k)\omega + \varphi \tag{5}$$

The time stamp of k^{th} downlink information about node B is $T_{B(3,k)}$, as shown in the following expression:

$$\mathrm{T}_{B(3,k)} = (T_{A(4,k)} - d - X_k)\omega + \varphi \tag{6}$$

Assuming $\{X_k\}_{k=1}^N$ and $\{Y_k\}_{k=1}^N$ are independent random variables whose means are 0 and variances are σ^2 with the Gaussian distribution and further assuming that delay d is a constant value and new variable $\omega' \triangleq 1/\omega$ is introduced, the maximum likelihood estimations of clock phase offset and clock frequency offset are as follows:

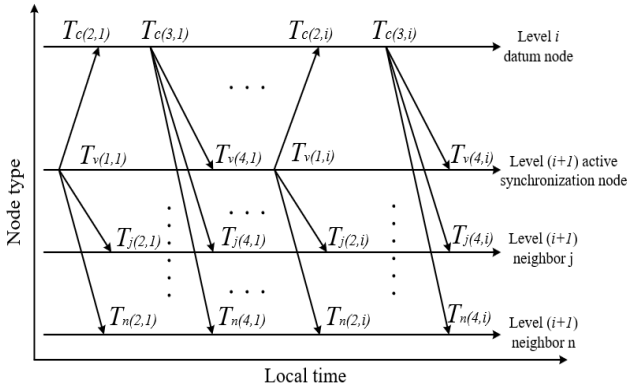

FIGURE 2. TSP-GDM synchronous message transmission model.

$$\varphi = \frac{\sum_{k=1}^{N} [\hat{\omega}'(T_{B(2,k)} + T_{B(3,k)}) - (T_{A(1,k)} + T_{A(4,k)})]}{2N\hat{\omega}'} \tag{7}$$

$$\omega = \frac{\sum_{k=1}^{N} [(T_{B(2,k)} - \hat{\varphi})^2 + (T_{B(3,k)} - \hat{\varphi})^2]}{\sum_{k=1}^{N} [(T_{A(1,k)} + d)(T_{B(2,k)} - \hat{\varphi}) + (T_{A(4,k)} - d)(T_{B(3,k)} - \hat{\varphi})]} \tag{8}$$

Based on the discussions above about data exchange between two nodes, the TSP-GDM algorithm will use the WSN monitoring network consisting of level i layer node and level $(i + 1)$ layer node to carry out the broadcast task with synchronous data message. Thus, the clock deviation estimation of component monitoring area nodes is realized.

The operation steps of TSP-GDM at i^{th} synchronizing cycle are as follows:

In the WSN monitoring network, a level $(i + 1)$ layer node (active synchronization node) sends a synchronous requirement message R_1 at the moment $T_{v(1,i)}$ and level i layer node(a datum node) will receive this message at the moment $T_{c(2,i)}$. Several level $(i + 1)$ layer neighbor nodes of active synchronization node will also receive this message at the moment $T_{j(2,i)}$. After datum node receives the message R_1, it will send a reply message A_1 (including time information $T_{c(2,i)}$) at the moment $T_{c(3,i)}$. The active synchronization node and its several level $(i + 1)$ layer neighbor nodes will receive this message at the moment $T_{v(4,i)}$ and $T_{j(4,i)}$ respectively. In Fig.2, multiple periodic time synchronization in the same synchronization process is described, among which time synchronization of the datum node and the active synchronization node belongs to the category of synchronization between senders and receivers.

For any neighbour node j in the i^{th} synchronizing cycle, its time parameter $T_{j(2,i)}$ should meet the formula:

$$\mathrm{T}_{\mathrm{j}(2,i)} = T_{v(v,j)} + w_{(v,j)}(T_{v(1,i)} - T_{v(1,i-k)}) + \Delta_{(v,j)} + d_{(v,j)} + X_{i(v,j)} \tag{9}$$

For node v and node j, $\omega_{(v,j)}$, $\Delta_{(v,j)}$, $d_{(v,j)}$, $X_{i(v,j)}$ represent clock frequency offset, clock phase offset, fixed transmission delay and random transmission delay between two nodes, and it is assumed that random transmission delay subject to Gauss distribution with mean value of 0 and variance of 0.5. According to the test result in [8], the clock offset of the node at receiving terminal approximately subject to the normal distribution whose mean value is 0 and standard deviation is $11.1\mu s$ (reliability is 99.8%), so that random transmission delay under Gaussian distribution is a reasonable hypothesis. This paper focuses on the situations of random transmission delay subject to Gaussian distribution. Likewise, for level i layer data node c, time parameter $T_{c(2,i)}$ should meet the formula as follows:

$$T_{c(2,i)} = T_{v(v,c)} + w_{(v,c)}(T_{v(1,i)} - T_{v(1,i-k)}) + \Delta_{(v,c)} + d_{(v,c)} + X_{i(v,c)} \quad (10)$$

From the operation of (9) and (10), we can get:

$$T_{c(2,i)} - T_{j(2,i)} = w_{(j,c)}(T_{v(1,i)} - T_{v(1,i-k)}) + \Delta_{(j,c)} + d_{(j,c)} + X_{i(j,c)} \quad (11)$$

Equation (11) can be expressed by a vector form:

$$X = H\theta + W \quad (12)$$

The definitions of every parameter in (12) are as follows:

$$\begin{cases} \theta = [\Delta_{(j,c)} \quad w_{(j,c)}]^T \\ H = \begin{pmatrix} 1 & 1 & \cdots & 1 \\ 0 & T_{v(1,2)} - T_{v(1,1)} & \cdots & T_{v(1,n)} - T_{v(1,n-k+1)} \end{pmatrix}^T \\ X[i] = T_{c(2,i)} - T_{j(2,j)} - d_{(j,c)} \end{cases}$$

The approximation of $X_{i(j,c)}$ in (11) is in line with the normal distribution whose average is 0 and variance is σ^2, then W is the Gaussian noise vector of $N \times 1$. According to the description of the theorem in [20], [21], [22], $\theta's$ linear minimum variance unbiased estimator (MVUE) is $(\mathrm{HTH})^{-1}\mathrm{HTX}$, and then the algorithm about θ is as shown in (13):

$$\begin{pmatrix} \hat{\Delta}^{(n)}_{(j,c)} \\ \hat{W}^{(n)}_{(j,c)} \end{pmatrix} = \begin{bmatrix} \sum_{i=s}^{n} D_i^2 \sum_{i=s}^{n} X[i] - \sum_{i=s}^{n} D_i \sum_{i=s}^{n} [D_i X[i]] \\ (n-s+1)\sum_{i=s}^{n} [D_i X[i]] - \sum_{i=s}^{n} D_i \sum_{i=s}^{n} X[i] \end{bmatrix} \times \frac{1}{(n-s+1)\sum_{i=s}^{n} D_i^2 - \left[\sum_{i=s}^{n} D_i\right]^2} \quad (13)$$

In (13) $D_i = T_{v(1,i)} - T_{v(1,s)}$, $i \in [s, n]$, parameter k is defined as synchronous round numbers included in a synchronization process (periodicity). When $1 \leq n \leq k$ and $n \in N+$, it means that current time synchronization is at the first stage, then $T_{v(1,n-k+1)} = T_{v(1,1)}$. When $n > k$, and $n \in N+$, it means new synchronization process is beginning. Considering the characteristics of data monitoring in wireless sensor networks, a periodic time synchronization strategy is usually ADOPTED. The synchronization interval is defined as τ, then (13) can be simplified as:

$$\begin{pmatrix} \hat{\Delta}^{(n)}_{(j,c)} \\ \hat{W}^{(n)}_{(j,c)} \end{pmatrix} = \begin{bmatrix} \dfrac{(4n-4s+2)\sum_{i=s}^{n} X[i] - 6\sum_{i=s}^{n}(i-s)X[i]}{(n-s+1)(n-s+2)} \\ \dfrac{12\sum_{i=s}^{n}(i-s)X[i] - 6(n-s)\sum_{i=s}^{n} X[i]}{(n-s)(n-s+2)(n-s+1)\tau} \end{bmatrix} \quad (14)$$

When $s = 1$, (14) should be changed to:

$$\begin{pmatrix} \hat{\Delta}^{(n)}_{(j,c)} \\ \hat{W}^{(n)}_{(j,c)} \end{pmatrix} = \begin{bmatrix} \dfrac{(4\mathrm{n}-2)\sum_{i=1}^{n} X[i] - 6\sum_{i=1}^{n}(i-1)X[i]}{n(n+1)} \\ \dfrac{12\sum_{i=1}^{n}(i-1)X[i] - 6(n-1)\sum_{i=1}^{n} X[i]}{n(n-1)(n+1)\tau} \end{bmatrix} \quad (15)$$

When $s = n - k + 1$, (14) should be changed to:

$$\begin{pmatrix} \hat{\Delta}^{(n)}_{(j,c)} \\ \hat{W}^{(n)}_{(j,c)} \end{pmatrix} = \begin{bmatrix} \dfrac{(4k-2)\sum_{i=n-k+1}^{n} X[i] - 6\sum_{i=n-k+1}^{n}(i-n+k-1)X[i]}{k(k+1)} \\ \dfrac{12\sum_{i=n-k+1}^{n}(i-n+k-1)X[i] - 6(k-1)\sum_{i=n-k+1}^{n} X[i]}{k(k-1)(k+1)\tau} \end{bmatrix} \quad (16)$$

After the calculation of estimation above, the estimation of local time of nth level i layer node c is as follows:

$$T^{(n)}_{(j,c)} = T_j + \Delta^{(n)}_{(j,c)} + w^{(n)}_{(j,c)}(T_j - T_{j(2,n-k)}) \quad (17)$$

According to [20] and (10), the Minimum Squared Error (MSE) between the clock phase offset $\theta_{(j,c)}$ and frequency offset $\omega_{(j,c)}$ is calculated as (18):

$$\begin{cases} MSE_{(\theta_{(j,c)})} = \dfrac{2\sigma^2(2n-1)}{n(n+1)} \\ MSE_{(\omega_{(j,c)})} = \dfrac{12\sigma^2}{n(n-1)(n+1)\tau^2} \end{cases} \quad (18)$$

where n is the number of synchronization wheels, σ^2 is the variance of random transmission delay and τ is the synchronization interval.

IV. SIMULATION AND RESULT ANALYSIS

A. EXPERIMENTAL ENVIRONMENT AND PARAMETER SETTINGS

If mathematics model of node clock is established by MATLAB, the relevant simulation conditions are as follows: the stability of crystal oscillator is defined as 50ppm, the phase offset range between the nodes as $-50 \sim 50\mu s$,

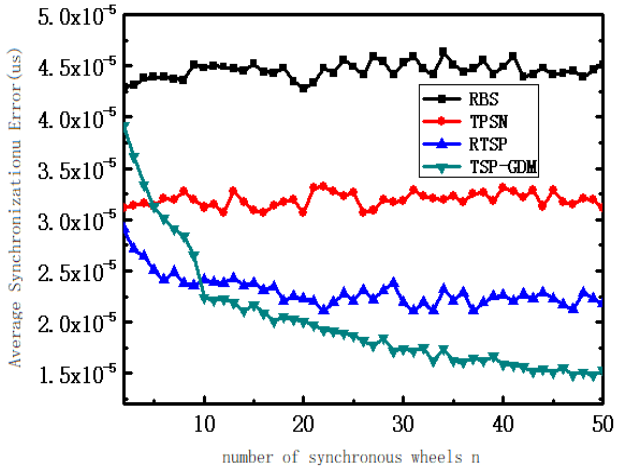

FIGURE 3. Average synchronization error curves of different algorithms.

the random error range of phase offset between the nodes as $-10 \sim 10\mu s$, the ideal interrupt count value at one second as 921600, the three selected nodes as datum node, active synchronization node and passive synchronization node respectively, the synchronization round number n as $0 \sim 50$, repetitions of the experiment as 1000, and average synchronization error is average value between the passive synchronization node and data node after 1000 repetitions of experiments.

B. ANALYSIS OF TIME SYNCHRONIZATION ACCURACY

Fig.3 shows the average synchronization error curves of TPSN, RBS, RTSP and TSP-GDM algorithms when number of synchronization wheels n is $0 \sim 50$. It can be seen that average synchronization error value of TPSN and RBS algorithms has been less influenced by parameter n because these two algorithms calculate time error value only by time stamp data of a single round. As RTSP and TSP-GDM algorithms utilize the statistics characteristics of multi-round time stamp data, when the number of round is larger (greater than 10), the average synchronization error is gradually declining. And the downtrend of TSP-GDM is more obvious than RTSP algorithm, namely, with the increase of the number of synchronization rounds, the average synchronization error of TSP-GDM is getting smaller than that of RTSP algorithm.

Table.1 has shown situations about single hop synchronization accuracy of several algorithms while number of synchronization wheels $n = 20$, and the unit of data in the table is microsecond. As is shown by the standard deviation in Table 1, TSP-GDM is relatively stable in synchronization accuracy, while TPSN and RBS algorithms are less stable in synchronization accuracy because they do not utilize the local time stamp statistical characteristics of synchronized nodes. It should be noted that the improvement of synchronization accuracy is usually at the expense of extra synchronization consumption, that is, without sufficient statistics of time stamps, it is difficult to achieve the synchronization accuracy of nodes.

TABLE 1. Comparison of single hop synchronization accuracy of different algorithms.

Synchronization Algorithm	Mean Error	Maximum Error	Minimum Error	Standard Deviation
TPSN	34.23	123.89	0.091	18.94
RBS	41.09	131.45	0.009	29.89
RTSP	22.78	105.42	0.027	17.45
TSP-GDM	18.52	77.22	0.011	14.68

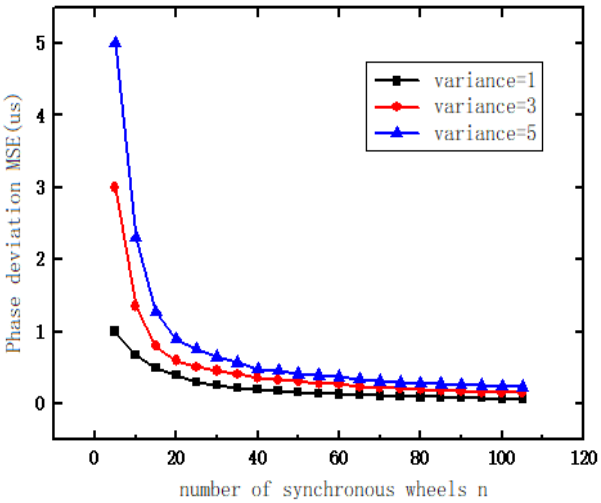

FIGURE 4. MSE curve of clock phase offset.

C. ANALYSIS OF MSE OF CLOCK OFFSET

Fig.4 shows the MSE curve of clock phase offset about n and σ^2, where $n \in [2, 100]$, $\sigma \in [1, 5]$ and $n, \sigma^2 \in N+$.

As is shown in Fig.4, with the increase of n and the decrease of σ^2, the MSE of clock phase shows a gradual downward trend, because when the number of synchronization rounds n takes a larger value, the relative clock changes between nodes will be estimated with more local time stamp data in (10). The link between the estimation and the $\hat{\theta}$ actual value θ of clock phase offset is as follows:

$$\hat{\theta} = \theta + f(X_i) \tag{19}$$

where the operation $f(\cdot)$ presents the primary operation on the random transmission delay. In this paper, based on the assumption that the random transmission delay $f(X_i)$ is subject to the Gaussian distribution with an average of 0 and a variance of 0.5, dependency exists between the clock offset estimation $\hat{\theta}$ and the value of random transmission delay X_i, that is, the MSE θ is relatively small when the value of X_i is small.

Fig.5 shows the MSE curve of clock frequency offset with respect to the number of synchronization wheels n, where $n \in [1, 21]$,$\sigma^2 = 1$ and $n \in N+$. As is shown in Fig.5, with the

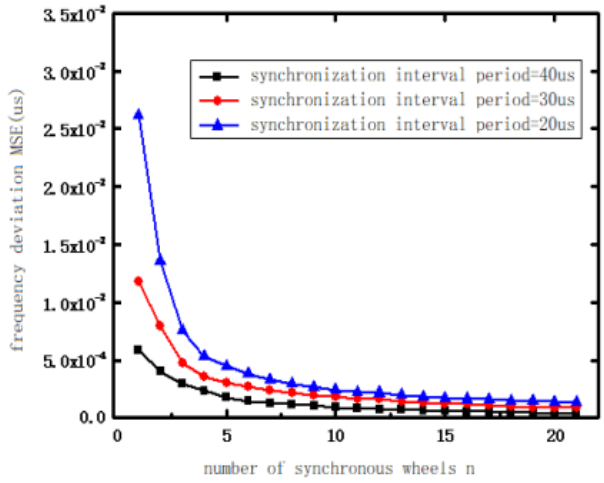

FIGURE 5. MSE curve of clock frequency offset.

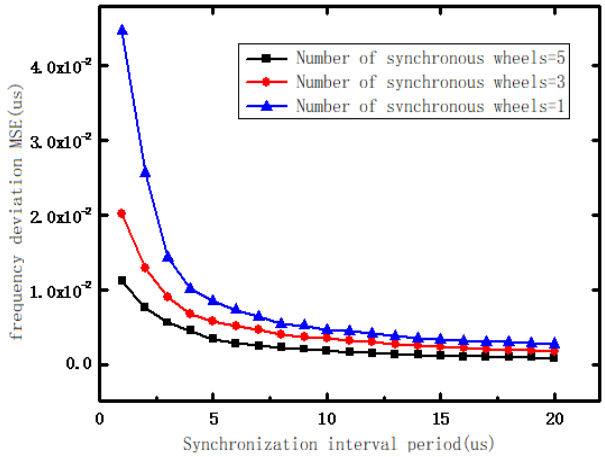

FIGURE 6. MSE curve of clock frequency offset.

increase of n, the MSE of clock frequency offset is declining, but the increase of the number of synchronization rounds n will introduce a larger synchronization message transmission cost.

Fig.6 shows the MSE curve of clock frequency offset with respect to synchronization interval τ. As is shown in Fig.6, with the increase of τ, the MSE of clock frequency offset shows a decreasing trend. The increase of τ is conducive to a more stable clock curve and thus reducing the MSE, but a larger value requires a longer synchronization period and leads to less synchronization efficiency in turn. From Fig.5 and Fig.6, n and τ value is not the bigger the better, so reasonable values of n and τ need to be reasonably set to meet the requirements of time synchronization.

D. COMPARATIVE ANALYSIS OF ENERGY CONSUMPTION OF ALGORITHMS

By increasing the number of nodes, i.e. setting 80, 100, 120, 140, 160, 180, 200, 220, 240, 260, 280, 300 nodes,

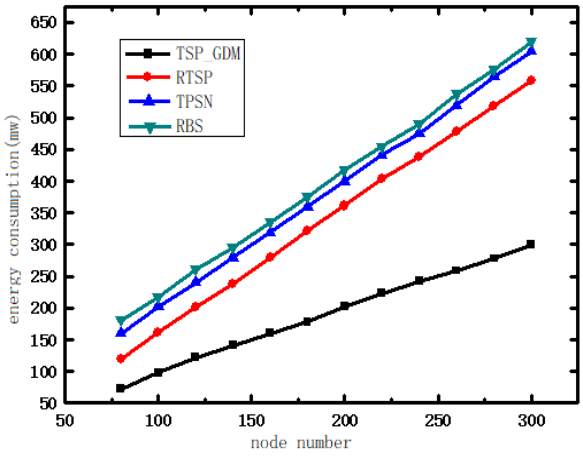

FIGURE 7. Energy consumption comparison of different algorithms.

simulation experiments are carried out on the network energy consumption to RBS, TPSN and RTSP algorithms. Fig.7 shows the comparison of energy consumption and its growth of the four algorithms under different nodes numbers. With the increase of the number of nodes, the amount of information exchanged between nodes decreases significantly compared with RBS, TPSN algorithm and RTSP algorithm. Therefore, it can be seen from Fig.7 that the energy consumption of the TSP-GDM algorithm is only half of that of the TPSN algorithm, while the energy consumption of the RBS algorithm is the largest in the same conditions. Meanwhile, With the continuous increase of the number of monitoring nodes, the trend of increasing energy consumption of TSP-GDM algorithm is more and more obvious, which is also one of the important advantages of the TSP-GDM algorithm.

V. CONCLUSION

In order to solve the clock offset problems under the conditions of WSN synchronization topology for monitoring the state of photovoltaic modules, TSP-GDM has been herein proposed. The algorithm utilizes the wireless broadcast characteristics of monitoring nodes in WSN to realize local time stamp sharing among nodes. An in-layer clock offset estimation algorithm is designed based on a Gaussian delay model in combination with a first-order linear clock. The simulation results indicate that the synchronization accuracy of the TSP-GDM algorithm for large-scale photovoltaic modules monitoring has increased 22.57 μs, 15.71 μs and 4.26 μs, respectively, comparing with RBS, TPSN and RTSP algorithm. The energy consumption of the TSP-GDM algorithm is only half of that of the TPSN algorithm. With the continuous increase of the number of monitoring nodes, the increasing trend of energy consumption of TSP-GDM algorithm is more moderate compared with other algorithms. Therefore, the proposed algorithm is applicable to monitoring the state of large-scale photovoltaic modules.

REFERENCES

[1] I. F. Akyildiz, W. Su, Y. Sankarasubramaniam, and E. Cayirci, "Wireless sensor networks: A survey," *Comput. Netw.*, vol. 38, no. 4, pp. 393–422, 2002.

[2] J. Elson and K. Römer, "Wireless sensor networks: A new regime for time synchronization," *ACM SIGCOMM Comput. Commun. Rev.*, vol. 33, no. 1, pp. 149–154, 2003.

[3] F. Sivrikaya and B. Yener, "Time synchronization in sensor networks: A survey," *IEEE Netw.*, vol. 18, no. 4, pp. 45–50, Jul./Aug. 2004.

[4] S. Ping, "Delay measurement time synchronization for wireless sensor networks," Intel Res. Berkeley Lab, Tech. Rep., 2003.

[5] M. Maróti, B. Kusy, and G. Simon, Á. Lédeczi, "The flooding time synchronization protocol," in *Proc. 2nd Int. Conf. Embedded Netw. Sensor Syst. (SenSys)*, Baltimore, MD, USA, 2004, pp. 39–49.

[6] S. Ganeriwal, R. Kumar, and M. B. Srivastava, "Timing-sync protocol for Sensor networks," in *Proc. 1st Int. Conf. Embedded Netw. Sensor Syst. (SenSys)*, Los Angeles, CA, USA, 2003, pp. 138–149.

[7] M. L. Sichitiu and C. Veerarittiphan, "Simple, accurate time synchronization for wireless sensor networks," in *Proc. IEEE Wireless Commun. Netw.*, Mar. 2003, pp. 1266–1273.

[8] J. Elson, L. Girod, and D. Estrin, "Fine-grained network time synchronization using reference broadcasts," in *Proc. 5th Symp. Oper. Syst. Design Implement.*, New York, NY, USA, vol. 36, 2002, pp. 147–163.

[9] S. PalChaudhuri, A. Saha, and D. B. Johnson, "Adaptive clock synchronization in sensor networks," in *Proc. 3th Int. Symp. Inf. Process. Sensor Netw.*, 2004, pp. 340–348.

[10] R. Leidenfrost and W. Elmenreich, "Firefly clock synchronization in an 802.15.4 wireless network," *EURASIP J. Embedded Syst.*, vol. 2009, no. 1, 2009, Art. no. 186406.

[11] T. Hao, R. Zhou, G. Xing, M. W. Mutka, and J. Chen, "WizSync: Exploiting Wi-Fi infrastructure for clock synchronization in wireless sensor networks," *IEEE Trans. Mobile Comput.*, vol. 13, no. 6, pp. 1379–1392, Jun. 2014.

[12] X.-P. Guan, X.-J. Zhang, and Z.-X. Liu, "Low-power clustering-based time synchronization mechanism for multi-hop WSN," (in Chinese), *Comput. Eng.*, vol. 36, no. 9, pp. 111–113, 2010.

[13] D. Djenouri, "R^4Syn: Relative referenceless receiver/receiver time synchronization in wireless sensor networks," *IEEE Signal Process. Lett.*, vol. 19, no. 4, pp. 175–178, Apr. 2012.

[14] M. K. Maggs, S. G. O'Keefe, and D. V. Thiel, "Consensus clock synchronization for wireless sensor networks," *IEEE Sensors J.*, vol. 12, no. 6, pp. 2269–2277, Jun. 2012.

[15] M. Akhlaq and T. R. Sheltami, "The recursive time synchronization protocol for wireless sensor networks," in *Proc. IEEE Sensors Appl. Symp.*, Brescia, Italy, Feb. 2012, pp. 1–6.

[16] R. Fengyuan, H. Haining, and L. Chuang, "Wireless sensor network," (in Chinese), *J. Softw.*, vol. 14, no. 7, pp. 1282–1291, 2003.

[17] Y. Sun, J. Zhang, Y. Sun, and Z. Fang, "Wireless self-organized sensor network," (in Chinese), *Chin. J. Sens. Actuators*, vol. 17, no. 2, pp. 331–335, 2004.

[18] W. Fuqiang, Z. Peng, and Y. Haibin, "A low overhead two-way time synchronization algorithm," (in Chinese), *Chin. J. Sci. Instrum.*, vol. 32, no. 6, pp. 1357–1363, 2011.

[19] M. Leng and Y. C. Wu, "On clock synchronization algorithms for wireless sensor networks under unknown delay," *IEEE Trans. Veh. Technol.*, vol. 59, no. 1, pp. 182–190, Jan. 2010.

[20] S. M. Kay, *Fundamentals of Statistical Signal Processing: Estimation Theory*. Upper Saddle River, NJ, USA: Prentice-Hall, 1993, pp. 71–80.

[21] L. T. Bruscato, T. Heimfarth, and E. P. de Freitas, "Enhancing time synchronization support in wireless sensor networks," *Sensors*, vol. 17, no. 12, p. 2956, 2017.

[22] H. Wang, L. Shao, M. Li, B. Wang, and P. Wang, "Estimation of clock skew for time synchronization based on two-way message exchange mechanism in industrial wireless sensor networks," *IEEE Trans. Ind. Informat.*, vol. 14, no. 11, pp. 4755–4765, Nov. 2018.

XIANBO SUN received the bachelor's degree in electrical engineering and automation from Hubei Minzu University, in 2000, and the master's degree in control theory and control engineering from the Wuhan University of Technology, in 2008. He is currently an Associate Professor and a Master Tutor. He is currently pursuing the Ph.D. degree. Doing multiple research work in the fields of control theory, control engineering, and industrial automation, he has been teaching various college courses, including microcomputer principle and interface technology, principle and application of single-chip computer, circuit principle, automatic control theory, multimedia technology, and so on. With more than ten papers published in domestic and foreign academic journals, including one monograph, he has chaired the Science and Technology Project of the Ministry of Industry, Natural Science Foundation projects, and two lateral projects. Besides, he is a core member of the Hubei Province Innovation Team and participates in two natural science foundation projects, two provincial department of education projects, and three provincial science and technology agency projects. He has received three national utility model patents, two national invention patents, and won two awards for Enshi Scientific and Technological Progress, one award for Hubei Provincial Scientific and Technological Progress, and the Enshi Second Youth Science and Technology Award.

YIXIN SU received the B.S. degree in process control from Wuhan University, Wuhan, China, in 1985, the M.S. degree in control theory and application from Southeast University, Nanjing, China, in 1988, and the Ph.D. degree in mechanical manufacturing and automation from the Huazhong University of Science and Technology, Wuhan, in 2006. He is currently a Professor and the Deputy Dean of the School of Automation, Wuhan University of Technology, Wuhan. His current research interests include intelligent controls, evolutionary computation, marine motion control, and cryptography technology for networks.

YONG HUANG , photograph and biography not available at the time of publication.

JIANJUN TAN , photograph and biography not available at the time of publication.

JINQIAO YI , photograph and biography not available at the time of publication.

TAO HU , photograph and biography not available at the time of publication.

LI ZHU , photograph and biography not available at the time of publication.